AGU PUBLICATIONS

Radio Science

RESEARCH ARTICLE
10.1002/2014RS005634

Key Points:
- Volume integral equation continuously inhomogeneous modeling is presented
- Lagrange-type modeling of dielectric properties in large elements is implemented
- Double-higher-order inhomogeneous elements are efficient in scattering analysis

Correspondence to:
B. M. Notaroš,
notaros@colostate.edu

Citation:
Chobanyan, E., M. M. Ilić, and B. M. Notaroš (2015), Lagrange-type modeling of continuous dielectric permittivity variation in double-higher-order volume integral equation method, *Radio Sci.*, *50*, 406–414, doi:10.1002/2014RS005634.

Received 3 DEC 2014
Accepted 24 APR 2015
Accepted article online 29 APR 2015
Published online 24 MAY 2015

Lagrange-type modeling of continuous dielectric permittivity variation in double-higher-order volume integral equation method

E. Chobanyan[1], M. M. Ilić[1,2], and B. M. Notaroš[1]

[1]Department of Electrical and Computer Engineering, Colorado State University, Fort Collins, Colorado, USA, [2]School of Electrical Engineering, University of Belgrade, Belgrade, Serbia

Abstract A novel double-higher-order entire-domain volume integral equation (VIE) technique for efficient analysis of electromagnetic structures with continuously inhomogeneous dielectric materials is presented. The technique takes advantage of large curved hexahedral discretization elements—enabled by double-higher-order modeling (higher-order modeling of both the geometry and the current)—in applications involving highly inhomogeneous dielectric bodies. Lagrange-type modeling of an arbitrary continuous variation of the equivalent complex permittivity of the dielectric throughout each VIE geometrical element is implemented, in place of piecewise homogeneous approximate models of the inhomogeneous structures. The technique combines the features of the previous double-higher-order piecewise homogeneous VIE method and continuously inhomogeneous finite element method (FEM). This appears to be the first implementation and demonstration of a VIE method with double-higher-order discretization elements and conformal modeling of inhomogeneous dielectric materials embedded within elements that are also higher (arbitrary) order (with arbitrary material-representation orders within each curved and large VIE element). The new technique is validated and evaluated by comparisons with a continuously inhomogeneous double-higher-order FEM technique, a piecewise homogeneous version of the double-higher-order VIE technique, and a commercial piecewise homogeneous FEM code. The examples include two real-world applications involving continuously inhomogeneous permittivity profiles: scattering from an egg-shaped melting hailstone and near-field analysis of a Luneburg lens, illuminated by a corrugated horn antenna. The results show that the new technique is more efficient and ensures considerable reductions in the number of unknowns and computational time when compared to the three alternative approaches.

1. Introduction

Both the finite element method (FEM) [*Jin*, 2002; *Ilić and Notaroš*, 2003; *Ilić et al*., 2009a; *Ansari-Oghol-Beig et al*., 2012] and the volume integral equation (VIE) method of moments (MOM) [*Schaubert et al*., 1984; *Notaroš and Popović*, 1998; *Sertel and Volakis*, 2002; *Kobidze and Shanker*, 2004; *Botha*, 2006; *Hasanovic et al*., 2007; *Järvenpää et al*., 2013] for modeling and analysis of electromagnetic (EM) scattering possess the inherent theoretical ability to directly treat continuously inhomogeneous dielectric materials. They allow that the dielectric parameters, permittivity (ε), and conductivity (σ), contained in the equivalent complex permittivity of the dielectric, can be an arbitrary function of spatial coordinates in the FEM or VIE computational domain, namely, $\varepsilon_e(\mathbf{r})$, with $\mathbf{r}$ standing for the position vector of a point in the adopted coordinate system. Converted to a numerical space, this theoretical ability means that a FEM or VIE technique or code should be able to actually implement $\varepsilon_e(\mathbf{r})$ as such and enable direct computation on volumetric discretization elements that include arbitrarily (continuously) inhomogeneous lossy dielectrics throughout individual elements. This is instead of carrying out FEM/VIE computations on piecewise homogeneous approximate models of the inhomogeneous structures, with $\varepsilon_e(\mathbf{r})$ replaced by appropriate piecewise constant approximations.

In addition to its theoretical relevance and interest, FEM or VIE numerical modeling with inhomogeneous volumetric discretization elements implementing $\varepsilon_e(\mathbf{r})$ variations has multiple practical applications in analysis of devices, systems, and phenomena that include continuously inhomogeneous materials in antennas, propagation, electronics, optics, bioelectromagnetics, inverse scattering, electromagnetic metamaterials, transformation electromagnetics/optics, etc., as outlined in *Ilić et al*. [2009b]. Moreover, if the direct FEM or VIE analysis of large continuously inhomogeneous regions in the structure is efficient, then one may even take advantage of a

"reverse" modeling procedure in some applications. Namely, one can approximate a given piecewise homogeneous structure (e.g., a medium composed of many thin homogeneous layers) by a continuously inhomogeneous medium (for a layered structure, generate a continuous interpolating ε_e profile through discrete values at centers of layers), and reduce the number of unknowns and accelerate the analysis by simulating the continuous model, in place of the actual structure.

In the FEM context, continuously inhomogeneous volume finite elements have been implemented and demonstrated in *Ilić et al*. [2009b]. It has also been discussed that modeling flexibility of continuously inhomogeneous finite elements can be fully exploited only if they can be made electrically large, which implies the use of higher-order field expansions within the elements. This is due to the fact that the elements within a low-order FEM technique must be electrically very small (on the order of a tenth of the wavelength in each dimension), and subdivision of the structure using such elements results in a discretization of the permittivity profiles as well, so elements can be treated as homogeneous; i.e., whether the actual $\varepsilon_e(\mathbf{r})$ function or its constant approximation is implemented throughout an element does not have much effect on the results. Thus, the treatment of finite elements as inhomogeneous can only be fully exploited if implemented in higher-order FEM modeling methodology that enables large geometrical elements (e.g., on the order of a wavelength in each dimension).

The VIE approach has equivalent capabilities for modeling of inhomogeneous dielectric materials as the FEM but has certain advantages over it; for example, VIE methods do not require additional unknowns associated with the termination of the computational FEM domain. In the VIE context, the possibility of using geometrical elements with continuous change of dielectric parameters throughout their volumes has been implicitly or explicitly stated, and/or the results of direct VIE analysis of continuously inhomogeneous dielectric structures, without using piecewise homogeneous approximate models, have been reported by *Popović and Notaroš* [1995], *Kim et al*. [2004], *Usner et al*. [2006], *Sheng et al*. [2012], *Tong* [2012], *Yang and Tong* [2012], *Yang et al*. [2013a, 2013b], and *Chobanyan et al*. [2013]. However, none of the works have provided much details about continuously inhomogeneous VIE implementations. More importantly, it also appears that there are no implementations and demonstrations of a higher-order VIE method employing large continuously inhomogeneous VIE elements, which may be referred to as the entire-domain or large-domain continuously inhomogeneous VIE analysis. A notable exception is the entire-domain analysis of continuously inhomogeneous dielectric scatterers in *Popović and Notaroš* [1995]. However, this method has limited accuracy and efficiency due to geometrical modeling using parallelepipeds (rectangular bricks), current modeling using divergence-nonconforming polynomial basis functions, and testing using the point-matching procedure. Another exception is a double-higher-order inhomogeneous VIE example in *Chobanyan et al*. [2013]. However, the results in this example, a continuously inhomogeneous dielectric spherical scatterer, aimed to show the capability of the proposed VIE technique to directly treat a continuously inhomogeneous dielectric, are generated in an "ad hoc" manner, with a special point-matching (zeroth-order) modeling of the continuously varying dielectric profile in spherical coordinates associated with the dielectric sphere, in which coordinates of the radial variation of dielectric permittivity inside the sphere are described. The ad hoc method used works only for this example, and is thus not described in the paper, and no general method for modeling of the continuously varying dielectric parameters within VIE elements is developed, implemented, or described.

This paper presents a novel double-higher-order entire-domain VIE technique for efficient analysis of EM structures with continuously inhomogeneous dielectric materials, based on Lagrange-type modeling of the continuously varying dielectric parameters within VIE elements. The technique uses Lagrange-type generalized curved parametric hexahedral elements of arbitrary geometrical orders for the approximation of geometry in conjunction with divergence-conforming hierarchical polynomial vector basis functions of arbitrary orders for the approximation of currents within the elements. Variations of $\varepsilon_e(\mathbf{r})$ are incorporated by means of the same Lagrange interpolating scheme used for defining element spatial coordinates. On one side, the technique represents a continuously inhomogeneous generalization of the double-higher-order (higher-order modeling of both the geometry and the current) VIE method in *Chobanyan et al*. [2013]. On the other side, it represents a VIE version of the continuously inhomogeneous FEM in *Ilić et al*. [2009b]. Overall, to the best of our knowledge, this is the first implementation and demonstration of a VIE method with double-higher-order discretization elements and conformal modeling of inhomogeneous dielectric materials embedded within elements that are also higher (arbitrary) order (with arbitrary material-representation orders within each curved and large VIE element). The new technique may thus even be referred to as a

triple-higher-order method. This paper also provides an elaborate and explicit discussion of continuously inhomogeneous VIE modeling.

The new technique has been validated and evaluated by comparisons with (i) the continuously inhomogeneous double-higher-order FEM technique [*Ilić et al*., 2009b], (ii) a piecewise homogeneous version of the double-higher-order VIE technique, and (iii) the commercial (piecewise homogeneous FEM) EM software ANSYS HFSS. The numerical examples demonstrate higher efficiency and considerable reductions in the number of unknowns and computational time with the new technique when compared to all three approaches (i)–(iii). The examples include two real-world applications involving continuously inhomogeneous permittivity profiles: scattering from a realistically shaped melting hailstone and near-field analysis of a Luneburg lens, illuminated by a corrugated horn antenna.

The paper is organized as follows: section 2 briefly outlines the general theory of a VIE and its double-higher-order discretization with a Galerkin-type MOM. Section 3 presents the modeling and implementation details of the proposed Lagrange-type continuous variation of $\varepsilon_e(\mathbf{r})$ within each VIE element. In section 4, the new technique is validated by various numerical examples.

2. Outline of the Volume Integral Equation Theory and Numerical Discretization

According to *Chobanyan et al*. [2013], the equation describing the EM problem of an arbitrarily shaped structure consisting of dielectric materials of the equivalent complex permittivity $\varepsilon_e = \varepsilon - j\sigma/\omega$ in a domain V, excited by a time-harmonic EM field of complex electric field intensity vector $\mathbf{E}_i$ and angular frequency ω, is given by

$$\frac{\mathbf{D}}{\varepsilon_e} - \omega^2\mu_0\int_V C\mathbf{D}g\,dV - \frac{1}{\varepsilon_0}\left[\int_V \nabla'\cdot(C\mathbf{D})\cdot\nabla g\,dV + \int_{S_d}\mathbf{n}\cdot(C\mathbf{D})\nabla g\,dS\right] = \mathbf{E}_i, \tag{1}$$

where $\mathbf{D}$ is the equivalent electric displacement vector, $\mathbf{D} = \varepsilon_e\mathbf{E}$, whose normal component is continuous ($\mathbf{n}\cdot\mathbf{D_1} = \mathbf{n}\cdot\mathbf{D_2}$) across the surfaces of abrupt discontinuity in ε_e, S_d. The electric contrast of the dielectric with respect to free space (background medium) is defined as $C = (\varepsilon_e - \varepsilon_0)/\varepsilon_e$, and g is the free-space Green's function.

In our discretization of equation (1) [*Chobanyan et al*., 2013], the computational domain is first geometrically tessellated using Lagrange-type generalized curved parametric hexahedra of arbitrary geometrical orders K_u, K_v, and K_w (K_u, K_v, $K_w \geq 1$), shown in Figure 1 and analytically described as [*Ilić and Notaroš*, 2003]

$$\begin{aligned}\mathbf{r}(u,v,w) &= \sum_{i=0}^{K_u}\sum_{j=0}^{K_v}\sum_{k=0}^{K_w}\mathbf{r}_{ijk}L_i^{K_u}(u)L_j^{K_v}(v)L_k^{K_w}(w),\\ L_i^{K_u}(u) &= \prod_{\substack{l=0\\ l\neq i}}^{K_u}\frac{u-u_l}{u_i-u_l}, \quad -1\leq u,v,w\leq 1,\end{aligned} \tag{2}$$

where $\mathbf{r}_{ijk} = \mathbf{r}(u_i, v_j, w_k)$ are the position vectors of interpolation nodes and $L_i^{K_u}$ represent Lagrange interpolation polynomials in the u coordinate, with u_l being the uniformly spaced interpolating nodes in u defined as $u_l = (2l - K_u)/K_u$, $l = 0, 1, \ldots, K_u$, and similarly for $L_j^{K_v}(v)$ and $L_k^{K_w}(w)$. Curvilinear hexahedral modeling facilitates volumetric meshes that can employ very large elements, which is consistent with the double-higher-order large-domain (entire-domain) VIE paradigm. Tetrahedral elements could be used (with appropriate local parent coordinate systems) as well but with limited flexibility in terms of large-domain modeling and generally larger numbers of unknowns when compared to hexahedral large-domain models. A key step in preprocessing for the analysis is generation of hexahedral meshes of higher (K_u, K_v, and) orders. Recently, commercial software meshing tools such as ANSYS ICEM CFD and csimsoft Trelis (formerly CUBIT) became available, which can automatically generate first- and second-order hexahedral meshes, and these are (K_u, K_v, and K_w) orders that suffice in most applications. For meshes of geometrical orders higher than two, one can

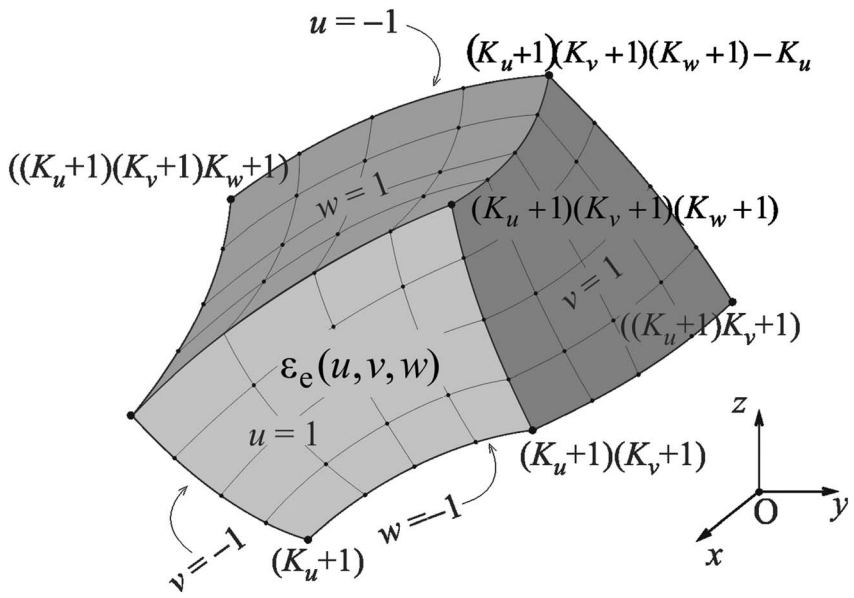

Figure 1. Generalized curved parametric hexahedral VIE element defined by equation (2), with a continuously varying dielectric profile given by equation (3).

use a technique that hierarchically converts a number of elements of geometrical orders K into an element of orders $K+1$.

Vector **D** inside every generalized hexahedron in the model is then expanded in terms of divergence-conforming hierarchical polynomial vector basis functions of arbitrary current-approximation orders N_u, N_v, and N_w (N_u, N_v, $N_w \geq 1$), as in *Chobanyan et al*. [2013]. After applying the Galerkin-type testing, we obtain a system of linear equations in a matrix form, where unknowns are the coefficients in the expansion for **D**.

3. Proposed Lagrange-Type VIE Modeling of Continuous Permittivity Variation

To implement continuous variations of material parameters, we utilize the already developed Lagrange interpolating scheme for defining spatial coordinates of an element in equation (2), which can be conveniently reused to govern the change of the equivalent complex permittivity ε_e within the hexahedral element, as follows:

$$\varepsilon_e(u,v,w) = \sum_{m=0}^{M_u}\sum_{n=0}^{M_v}\sum_{p=0}^{M_w} \varepsilon_{e,mnp} L_m^{M_u}(u) L_n^{M_v}(v) L_p^{M_w}(w), \quad -1 \leq u,v,w \leq 1\,, \tag{3}$$

where $\varepsilon_{e,mnp} = \varepsilon_e(u_m, v_n, w_p)$ are the permittivity values at the points defined by $(M_u+1)(M_v+1)(M_w+1)$ position vectors of spatial interpolation nodes $\mathbf{r}(u_m, v_n, w_p)$, with M_u, M_v, and M_w (M_u, M_v, $M_w \geq 1$) standing for arbitrary material-representation polynomial orders within the VIE element in Figure 1, similarly to *Ilić et al*. [2009b]. For example, in the case of $M_u = M_v = M_w = 1$, ε_e is a trilinear function throughout the element volume, governed by the given fixed values at eight points—hexahedron vertices. If $M_u = M_v = M_w = 2$, then the inputs are values for ε_e at 27 interpolation nodes, and the corresponding profiles are triquadratic functions and so on. Geometrical-mapping orders (K_u, K_v, K_w), current-expansion orders (N_u, N_v, N_w), and material-representation orders (M_u, M_v, M_w) are entirely independent from each other, and the three sets of parameters of a double-higher-order inhomogeneous model can be combined independently for the best overall performance of the method. Furthermore, all of the parameters can be adopted anisotropically in different directions within an element and nonuniformly from element to element in a model.

Starting with equation (1) and having in mind the general VIE expression for generalized Galerkin MOM impedances (the system matrix elements) using magnetic vector and electric scalar Lorenz potentials in

Chobanyan et al. [2013], we derive the following expression for the matrix entry corresponding to the testing functions $\mathbf{f}_m$ and basis functions $\mathbf{f}_n$ defined on the mth and nth inhomogeneous double-higher-order hexahedral VIE elements (V_m and V_n), respectively, in the model

$$\begin{aligned} Z_{mn} &= \int_{V_m} \frac{1}{\varepsilon_{em}} \mathbf{f}_m \cdot \mathbf{f}_n \mathrm{d}V_m - \omega^2 \mu_0 \int_{V_m} \mathbf{f}_m \int_{V_n} \mathbf{f}_n C_n g \mathrm{d}V_n \mathrm{d}V_m \\ &\quad - \frac{1}{\varepsilon_0} \left[\int_{V_m} \mathbf{f}_m \int_{V_n} \nabla' \cdot (C_n \mathbf{f}_n) \cdot \nabla g \mathrm{d}V_n \mathrm{d}V_m + \int_{V_m} \mathbf{f}_m \int_{S_n} \mathbf{n} \cdot (C_n \mathbf{f}_n) \nabla g \mathrm{d}\mathbf{S}_n \mathrm{d}V_m \right] \\ &= \int_{V_m} \frac{1}{\varepsilon_{em}} \mathbf{f}_m \cdot \mathbf{f}_n \mathrm{d}V_m - \omega^2 \mu_0 \int_{V_m} \mathbf{f}_m \int_{V_n} \mathbf{f}_n C_n g \mathrm{d}V_n \mathrm{d}V_m + \frac{1}{\varepsilon_0} \int_{V_m} \nabla \cdot \mathbf{f}_m \int_{V_n} C_n \nabla \cdot \mathbf{f}_n g \mathrm{d}V_n \mathrm{d}V_m \\ &\quad + \frac{1}{\varepsilon_0} \int_{V_m} \nabla \cdot \mathbf{f}_m \int_{V_n} \mathbf{f}_n \cdot \nabla C_n g \mathrm{d}V_n \mathrm{d}V_m + \frac{1}{\varepsilon_0} \int_{V_m} \nabla \cdot \mathbf{f}_m \int_{S_n} C_n \mathbf{f}_n \cdot \mathbf{n} g \mathrm{d}V_n \mathrm{d}V_m \\ &\quad - \frac{1}{\varepsilon_0} \int_{S_m} \mathbf{f}_m \cdot \mathbf{n} \int_{V_n{}^n} C_n \nabla \cdot \mathbf{f}_n g \mathrm{d}V_n \mathrm{d}S_m - \frac{1}{\varepsilon_0} \int_{S_m} \mathbf{f}_m \cdot \mathbf{n} \int_{V_n{}^n} \mathbf{f}_n \cdot \nabla C_n g \mathrm{d}V_n \mathrm{d}S_m \\ &\quad - \frac{1}{\varepsilon_0} \int_{S_m} \mathbf{f}_m \cdot \mathbf{n} \int_{S_n} C_n \mathbf{f}_n \cdot \mathbf{n} \mathrm{d}S_n \mathrm{d}S_m \end{aligned} \quad , \tag{4}$$

with S_m and S_n being the surfaces of the mth and nth elements, respectively, oriented outward. If ε_{em} and ε_{en} are constant, all terms including ∇C_n are vanishing, $1/\varepsilon_{em}$ and C_n can be taken outside the respective integrals, and the final expression in equation (4) reduces to its piecewise homogeneous version, with both elements being filled with homogeneous dielectrics, in *Chobanyan et al.* [2013]. For continuously inhomogeneous elements, ∇C_n in the integrals is calculated as

$$\nabla C_n = \frac{\partial C_n}{\partial u} \frac{\partial \mathbf{r}}{\partial u} + \frac{\partial C_n}{\partial v} \frac{\partial \mathbf{r}}{\partial v} + \frac{\partial C_n}{\partial w} \frac{\partial \mathbf{r}}{\partial w}, \quad \frac{\partial C_n}{\partial u} = \frac{\partial}{\partial u} \left(\frac{\varepsilon_e - \varepsilon_0}{\varepsilon_e} \right) = \frac{\varepsilon_0}{\varepsilon_e^2} \frac{\partial \varepsilon_e}{\partial u}, \tag{5}$$

with similar expressions for $\partial C_n/\partial v$ and $\partial C_n/\partial w$. With $\mathbf{r}$ and ε_e within each element represented as in equations (2) and (3), respectively, the calculation of partial derivatives in equation (5) is a matter of simple analytical differentiation of Lagrange polynomials. The singular integrals in equation (4) are evaluated by a singularity extraction technique described in *Chobanyan et al.* [2013], where the technique for generation of the generalized Galerkin impedances (for homogeneous elements) is presented in detail as well. The numerical integration is carried out using the Gauss-Legendre integration formula with orders generally adopted as NGL = $N+2$, where N are the current-approximation orders in the element, which is in accordance with the guidelines established in *Klopf et al.* [2012].

4. Numerical Results

All simulations are performed on a PC with Intel® Core™ i7 CPU 960 processor at 3.2 GHz, 24 Gb of random access memory (RAM), and 64 bit Windows 7 operating system. The current version of the presented continuously inhomogeneous double-higher-order VIE technique is a classical MOM code, that is not accelerated in any way and is not parallelized, with the final matrix equation being solved utilizing a direct solver, based on lower upper factorization (with full matrix storage). Hence, the computational (CPU) complexities of the matrix filling and matrix solution are O(N^2) and O(N^3), respectively, and the memory consumption scales as O(N^2). In all examples, the choice of the current-expansion orders (N_u, N_v, and N_w) is made based on *Klopf et al.* [2012].

4.1. Continuously Inhomogeneous Spherical Dielectric Scatterer

As the first example illustrating the efficiency of the proposed technique in modeling of continuously inhomogeneous structures, we consider a lossless ($\sigma = 0$) spherical dielectric ($\mu_r = 1$) scatterer, of radius $a = 10$ cm, situated in free space and illuminated by a uniform plane wave of frequency $f = 1.3$ GHz, impinging from $\theta_{inc} = 0°$ and $\phi_{inc} = 0°$ directions. The relative permittivity of the sphere is a linear function of a radial coordinate r with the coordinate origin coinciding with the center of the sphere, $\varepsilon_r(r) = 6 - 5r/a$, as depicted in the inset of Figure 2. The sphere is modeled by seven curvilinear hexahedral elements of the second geometrical order ($K_u = K_v = K_w = 2$); in specific, the model consists of the central sphere-like hexahedron of radius

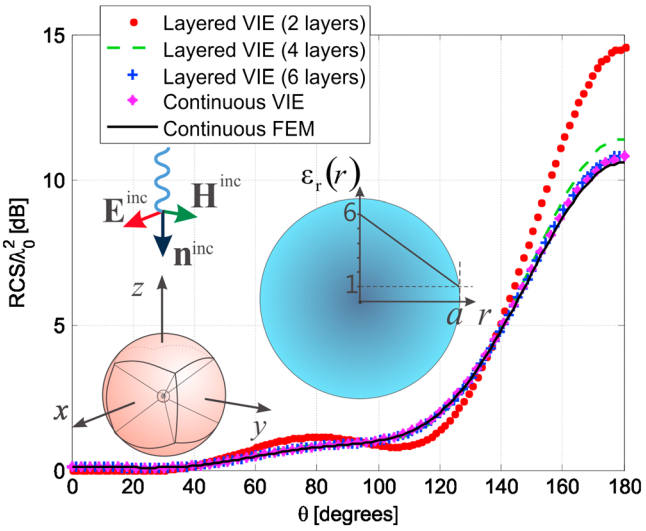

Figure 2. Normalized bistatic radar cross section (RCS) of an inhomogeneous dielectric spherical scatterer (shown in the inset): comparison of the results obtained by the proposed continuously inhomogeneous double-higher-order VIE technique, layered VIE solutions on three different piecewise homogeneous double-higher-order models, and continuously inhomogeneous double-higher-order FEM results.

$a/20$ and six "cushion-like" hexahedra between the central sphere and the scatterer surface. The current-approximation orders are $N_u = N_v = N_w = 2$ for the small central element and $N_u = N_v = N_w = 4$ for all the "cushions," resulting in a total of $N_{\text{unkn}}^{\text{VIE}} = 1380$ unknowns. The permittivity $\varepsilon_e = \varepsilon_r \varepsilon_0$ inside the curved elements is represented as a Lagrange polynomial function of material-representation orders $M_u = M_v = M_w = 1$.

Validation and evaluation of the continuously inhomogeneous VIE model is carried out in comparison with VIE simulations of piecewise homogeneous approximate models of the structure and a continuously inhomogeneous FEM as a reference solution. Three different piecewise homogeneous models are constructed for the comparison, where the inhomogeneous cushion-like elements are replaced by $N_L = 2$, 4, and 6 layers, respectively, of thin homogeneous cushions of geometrical orders $K_u = K_v = K_w = 2$ and current-approximation orders $N_u = N_v = N_w = 3$. Figure 2 shows the bistatic radar cross section (RCS) of the sphere, normalized to λ_0^2 (λ_0 being the free-space wavelength), in a characteristic plane ($\phi = 90°$). It can be observed that with increasing N_L, solutions obtained using the piecewise homogeneous models converge to the results of the continuously inhomogeneous VIE analysis, as well as that the continuous VIE solution accurately matches the reference continuous FEM solution [*Ilić et al.*, 2009b], utilizing the same continuously inhomogeneous large curved hexahedral elements, but with completely different field equations and numerical procedure. In addition, as can be concluded from Table 1, the continuous VIE approach demonstrates advantages in both the number of unknowns and the computational time in comparison with the most precise piecewise homogeneous layered VIE model, with $N_L = 6$.

4.2. Realistic Scattering Modeling of an Egg-Shaped Melting Hailstone

The second example illustrates a real-life application of the technique, where we consider an egg-shaped melting hailstone with a linear radial variation of the relative equivalent permittivity which changes from $\varepsilon_{er} = 20.71 - j5.23$ (wet hail), at the surface, to $\varepsilon_{er} = 3.14 - j0.004$ (dry hail) [*Aydin et al.*, 1997], at the center of the object, as depicted in the inset of Figure 3. Similarly to the first example, the hailstone is modeled by only seven inhomogeneous curvilinear hexahedral VIE elements with $K_u = K_v = K_w = 2$, $N_u = N_v = N_w = 6$, $M_u = M_v = M_w = 2$, and $N_{\text{unkn}}^{\text{VIE}} = 5076$. The computational time is $T_{\text{total}}^{\text{VIE}} = T_{\text{filling}}^{\text{VIE}} + T_{\text{solving}}^{\text{VIE}} = 1256\text{ s} + 30\text{ s} = 1286\text{ s}$ per frequency point, and the RAM consumption is 412.3 Mb. Validation of the inhomogeneous double-higher-order VIE model is carried out in comparison with the solution obtained by the inhomogeneous double-higher-order FEM [*Ilić et al.*, 2009b]. The FEM simulation requires $N_{\text{unkn}}^{\text{FEM}} = 5646$ unknowns,

Table 1. Comparison of the Number of Unknowns, Computational Time, and Memory (RAM) Usage for the Continuous VIE and Layered VIE Solutions in Figure 2

	Number of Unknowns	Matrix Filling Time (s)	Matrix Solving Time (s)	RAM (Mb)
Continuous VIE	1380	138	2	30.5
Layered VIE $N_L = 2$	1215	45	1	23.6
Layered VIE $N_L = 4$	2295	150	5	84.3
Layered VIE $N_L = 6$	3375	315	12	182.3

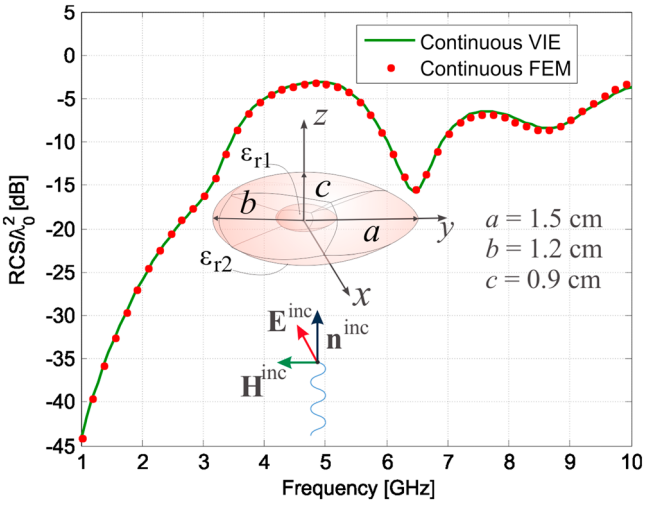

Figure 3. Normalized monostatic RCS of an egg-shaped continuously inhomogeneous melting hailstone model (shown in the inset): comparison of continuously inhomogeneous double-higher-order VIE and FEM solutions.

$T^{FEM} = 5086$ s of computational time, and 365.9 Mb of RAM. Shown in Figure 3 is the normalized monostatic RCS of the hailstone for the wave incident from the negative z direction, computed in the frequency range from 1 GHz to 10 GHz, where we observe an excellent agreement of the results obtained by the two numerical methods.

4.3. Near-Field Analysis of a 10 Wavelength Luneburg Lens Illuminated by a Corrugated Horn Antenna

As the last example, consider a Luneburg lens, in the form of a dielectric sphere with relative permittivity varying radially from 2, at the sphere center, to 1, at the surface, that is, $\varepsilon_r(r) = 2 - (r/R)^2$, where R is the radius of the lens. The lens is $10\lambda_0$ in diameter and is illuminated by a corrugated horn antenna made of a perfect electric conductor (PEC), as shown in Figure 4. The lens is modeled by 112 inhomogeneous curvilinear hexahedral VIE elements with $K_u = K_v = K_w = 2$, $N_u = N_v = N_w = 4$, and $M_u = M_v = M_w = 2$, and the corrugated horn antenna model consists of 124 quadrilateral PEC patches with $K_u = K_v = 1$ and $N_u = N_v = 3$. In this example, the VIE in equation (1) for the lens is coupled with the surface integral equation (SIE) for the horn antenna, resulting in a hybrid VIE-SIE system of integral equations, which are discretized and solved simultaneously, as described in *Chobanyan et al.* [2013]. With the use of symmetry (only one fourth of the lens-horn structure is modeled), the VIE-SIE discretization of the model requires a total of $N_{unkn}^{VIE\text{-}SIE} = 24,501$ unknowns; $T_{total}^{VIE\text{-}SIE} = T_{filling}^{VIE\text{-}SIE} + T_{solving}^{VIE\text{-}SIE} = 11,415$ s $+3230$ s $= 14,645$ s of computational time; and 9.6 Gb of RAM.

We validate the VIE-SIE model by demonstrating the lens effect and comparing the near-field results with those obtained by the commercial FEM EM software ANSYS HFSS. The simulated normalized real part of the y component of the electric field vector in the xOz plane passing through the lens is shown in Figure 5. Both simulations, by the VIE-SIE and HFSS, clearly demonstrate the effect of the lens while cross-validating each other (acknowledging the slight differences in the color coding used in the two codes and difference in excitation modeling, which in HFSS is a wave port and in VIE-SIE is a point-delta generator). In addition, the proposed continuously inhomogeneous VIE-SIE technique demonstrates better computational efficiency in comparison with the HFSS simulation, which, with only one fourth of the structure in Figure 4 modeled using symmetry, requires 1,052,815 homogeneous tetrahedra; 252 triangles; $N_{unkn}^{HFSS} = 6,678,731$ unknowns; $T^{HFSS} = 28,297$ s of computational time (for a single adaptive pass); and 22.8 Gb of RAM; this is

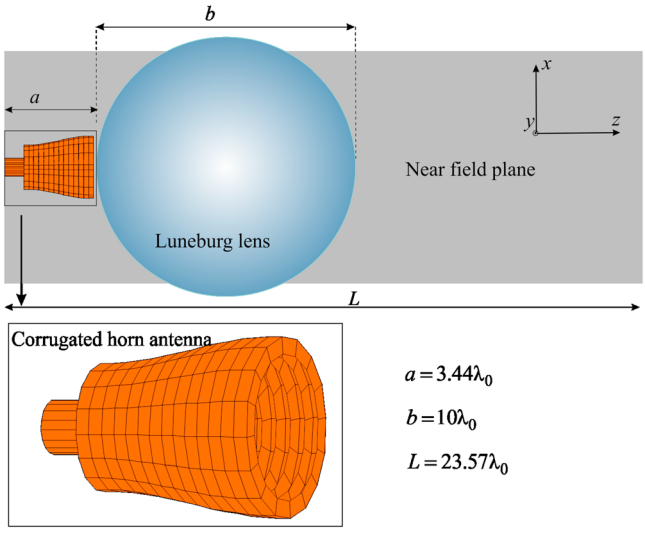

Figure 4. VIE-SIE analysis of a 10 λ_0 radially continuously inhomogeneous dielectric Luneburg lens illuminated by a corrugated horn PEC antenna.

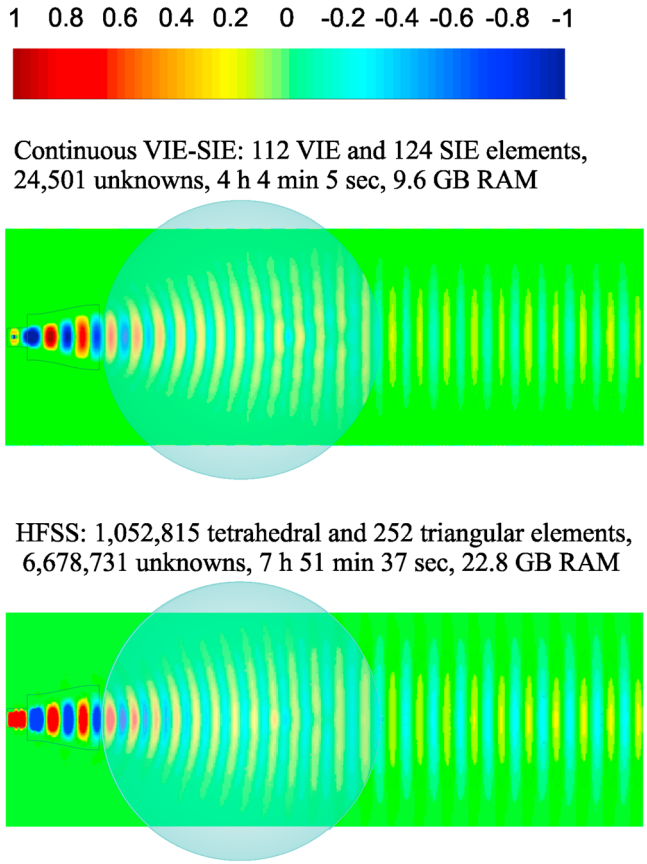

Figure 5. Near electric field of a 10 λ_0 Luneburg lens illuminated by a corrugated horn antenna: comparison of the continuously inhomogeneous double-higher-order VIE-SIE solution and the results obtained by the commercial (piecewise homogeneous FEM) code ANSYS HFSS.

approximately 1.93 times slower and 2.48 times more memory consuming than the VIE-SIE computation.

5. Conclusions

This paper has presented a novel double-higher-order entire-domain VIE technique for efficient analysis of scattering from continuously inhomogeneous dielectric bodies. Special Lagrange-type generalized curved parametric hexahedra with continuous variations of dielectric parameters have been utilized for geometrical tessellation as part of VIE modeling. The general expression for computation of the Galerkin MOM matrix for inhomogeneous double-higher-order hexahedral VIE elements has been derived and implemented. The technique combines the features of the previously published double-higher-order VIE method and the continuously inhomogeneous FEM. To the best of our knowledge, this is the first implementation and demonstration of continuously inhomogeneous tessellation elements in a double-higher-order VIE approach with conformal modeling of inhomogeneous dielectric materials embedded within elements that are also higher order, with arbitrary material-representation orders within each curved and large VIE element.

The new technique has been validated and evaluated by comparisons with a continuously inhomogeneous double-higher-order FEM technique, a piecewise homogeneous version of the double-higher-order VIE technique, and the commercial piecewise homogeneous FEM code HFSS. The examples have included scattering from an inhomogeneous sphere and an egg-shaped melting hailstone and near-field analysis of a Luneburg lens, illuminated by a corrugated horn antenna. The new technique has been found to be more efficient and to ensure considerable reductions in the number of unknowns and computational time when compared to the three alternative approaches. In addition, it should be noted that, in general, implementation of $\varepsilon_e(\mathbf{r})$ as a function of the position in each geometrical element becomes efficient when electrically large elements are utilized. Therefore, double-higher-order discretization in conjunction with the continuously inhomogeneous VIE is more practical for application purposes than its low-order counterparts.

Acknowledgments
The data for this paper can be obtained upon request to Elene Chobanyan, Electromagnetics Laboratory, Department of Electrical and Computer Engineering, Colorado State University (elene.chobanyan@colostate.edu). This work at Colorado State University was supported by the National Science Foundation under grants ECCS-1002385 and AGS-1344862 and by the Serbian Ministry of Education, Science, and Technological Development under grant TR-32005.

References

Ansari-Oghol-Beig, D., J. Wang, Z. Peng, and J.-F. Lee (2012), A universal array approach for finite elements with continuously inhomogeneous material properties, *IEEE Trans. Antennas Propag.*, *60*(10), 4745–4756, doi:10.1109/TAP.2012.2207310.

Aydin, K., S. H. Park, and T. M. Walsh (1997), Bistatic dual-polarization scattering from rain and hail at S- and C-band frequencies, *J. Atmos. Oceanic Technol.*, *15*, 1110–1121, doi:10.1175/1520-0426(1998)015<1110:BDPSFR>2.0.CO;2.

Botha, M. M. (2006), Solving the volume integral equations of electromagnetic scattering, *J. Comput. Phys.*, *218*(1), 141–158, doi:10.1016/j.jcp.2006.02.004.

Chobanyan, E., M. M. Ilić, and B. M. Notaroš (2013), Double-higher-order large-domain volume/surface integral equation method for analysis of composite wire-plate-dielectric antennas and scatterers, *IEEE Trans. Antennas Propag.*, *61*(12), 6051–6063, doi:10.1109/TAP.2013.2281360.

Hasanovic, M., C. Mei, J. R. Mautz, and E. Arvas (2007), Scattering from 3-D inhomogeneous chiral bodies of arbitrary shape by method of moments, *IEEE Trans. Antennas Propag.*, *55*(6), 1817–1825, doi:10.1109/TAP.2007.898590.

Ilić, M. M., and B. M. Notaroš (2003), Higher order hierarchical curved hexahedral vector finite elements for electromagnetic modeling, *IEEE Trans. Microwave Theory Tech.*, *51*(3), 1026–1033, doi:10.1109/TMTT.2003.808680.

Ilić, M. M., M. Djordjević, A. Ž. Ilić, and B. M. Notaroš (2009a), Higher order hybrid FEM-MOM technique for analysis of antennas and scatterers, *IEEE Trans. Antennas Propag.*, *57*(5), 1452–1460, doi:10.1109/TAP.2009.2016725.

Ilić, M. M., A. Ž. Ilić, and B. M. Notaroš (2009b), Continuously inhomogeneous higher order finite elements for 3-D electromagnetic analysis, *IEEE Trans. Antennas Propag.*, *57*(9), 2798–2803, doi:10.1109/TAP.2009.2027350.

Järvenpää, S., J. Markkanen, and P. Ylä-Oijala (2013), Broadband multilevel fast multipole algorithm for electric-magnetic current volume integral equation, *IEEE Trans. Antennas Propag.*, *61*(8), 4393–4397, doi:10.1109/TAP.2013.2262113.

Jin, J. M. (2002), *The Finite Element Method in Electromagnetics*, 2nd ed., John Wiley, New York.

Kim, O. S., P. Meincke, O. Breinbjerg, and E. Jørgensen (2004), Method of moments solution of volume integral equations using higher-order hierarchical Legendre basis functions, *Radio Sci.*, *39*, RS5003, doi:10.1029/2004RS003041.

Klopf, E. M., N. J. Šekeljić, M. M. Ilić, and B. M. Notaroš (2012), Optimal modeling parameters for higher order MOM-SIE and FEM-MOM electromagnetic simulations, *IEEE Trans. Antennas Propag.*, *60*(6), 2790–2801, doi:10.1109/TAP.2012.2194669.

Kobidze, G., and B. Shanker (2004), Integral equation based analysis of scattering from 3-D inhomogeneous anisotropic bodies, *IEEE Trans. Antennas Propag.*, *52*(10), 2650–2658, doi:10.1109/TAP.2004.834439.

Notaroš, B. M., and B. D. Popović (1998), Large-domain integral-equation method for analysis of general 3-D electromagnetic structures, *IEE Proc. - Microwaves, Antennas Propag.*, *145*(6), 491–495, doi:10.1049/ip-map:19982385.

Popović, B. D., and B. M. Notaroš (1995), Entire-domain polynomial approximation of volume currents in the analysis of dielectric scatterers, *IEE Proc. - Microwaves, Antennas Propag.*, *142*(3), 207–212, doi:10.1049/ip-map:19951825.

Schaubert, D. H., D. R. Wilton, and A. W. Glisson (1984), A tetrahedral modeling method for electromagnetic scattering by arbitrarily shaped inhomogeneous dielectric bodies, *IEEE Trans. Antennas Propag.*, *AP-32*, 77–85, doi:10.1109/TAP.1984.1143193.

Sertel, K., and J. L. Volakis (2002), Method of moments solution of volume integral equations using parametric geometry modeling, *Radio Sci.*, *37*(1), 1010, doi:10.1029/2000RS002597.

Sheng, W. T., Z. Y. Zhu, and M. S. Tong (2012), On the method of moments solution for volume integral equation with inhomogeneous dielectric media, *IEEE Antennas Wireless Propag. Lett.*, *11*, 1154–1157, doi:10.1109/LAWP.2012.2219573.

Tong, M. S. (2012), Meshfree solutions of volume integral equations for electromagnetic scattering by anisotropic objects, *IEEE Trans. Antennas Propag.*, *60*(9), 4249–4258, doi:10.1109/TAP.2012.2207052.

Usner, B. C., K. Sertel, M. A. Carr, and J. L. Volakis (2006), Generalized volume-surface integral equation for modeling inhomogeneities within high contrast composite structures, *IEEE Trans. Antennas Propag.*, *54*(1), 68–75, doi:10.1109/TAP.2005.861579.

Yang, K., and M. S. Tong (2012), A meshless scheme for solving volume integral equations with inhomogeneous media, *IEEE Antennas Propag. Soc. Int. Symp. (APSURSI)*, *8–14*, 1–2, doi:10.1109/APS.2012.6348562.

Yang, K., J. C. Zhou, W. T. Sheng, Z. T. Zhu, and M. S. Tong (2013a), Electromagnetic analysis for inhomogeneous interconnect and packaging structures based on volume-surface integral equations, *IEEE Trans. Compon. Packag. Manuf. Technol.*, *3*(8), 1364–1371, doi:10.1109/TCPMT.2013.2241436.

Yang, K., J. C. Zhou, W. T. Sheng, Z. T. Zhu, and M. S. Tong (2013b), Efficient Nyström solutions of electromagnetic scattering by composite objects with inhomogeneous anisotropic media, *IEEE Trans. Antennas Propag.*, *61*(10), 5328–5332, doi:10.1109/TAP.2013.2272671.